A simplified method for predicting the settlement of circular footings on multi-layered geocell-reinforced non-cohesive soils

S.N. Moghaddas Tafreshi [1], T. Shaghaghi[2], Gh. Tavakoli Mehrjardi[3], A.R. Dawson[4], M. Ghadrdan[5]

[1]*Corresponding Author, Department of Civil Engineering, K.N. Toosi University of Technology, Tehran, Iran. Tel: +982188779473; Fax: +982188779476; E-mail address: nas_moghaddas@kntu.ac.ir*

[2]*MSc graduated, Department of Civil Engineering, K.N. Toosi University of Technology, Tehran, Iran. Tel: +982188779473; Fax: +982188779476; E-mail address: tahereh.shaghaghi@gmail.com*

[3]*Department of Civil Engineering, Faculty of Engineering, University of Kharazmi, Tehran, Iran E-mail address: ghtavakoli@khu.ac.ir*

[4]*Nottingham Transportation Engineering Centre, University of Nottingham, Nottingham, UK. Tel: +441159513902; Fax: +441159513909; E-mail address: andrew.dawson@nottingham.ac.uk*

[5]*MSc graduated, Department of Civil Engineering, K.N. Toosi University of Technology, Tehran, Iran. Tel: +982188779473; Fax: +982188779476; E-mail address:mg1365@gmail.com*

Abstract: Multiple layers of geosynthetic reinforcement, placed below foundations or in the supporting layers of road pavements, can improve section performance through several mechanisms, leading to reduction in stresses and deformations. This paper aims to present a new analytical solution, based on the theory of multi-layered soil system to estimate the pressure-settlement response of a circular footing resting on such foundations, specifically those containing geocell layers. An analytical model that incorporates the elastic characteristics of soil and reinforcement is developed to predict strain and confining pressure propagated throughout an available multi-layer system, is proposed. A modified elastic method has been used to back-calculate the elastic modulus in terms of strain and confining pressure with materials data extracted from triaxial tests on unreinforced and geocell-reinforced soil samples. The proposed model has been validated by results of plate load tests on unreinforced and geocell-reinforced foundation beds. The comparisons between the results of the plate load tests and proposed analytical method reflected a satisfactory accuracy and consistency, especially at expected, practical, settlement ratios. Furthermore, to have a better assessment of geocell-reinforced foundations' behavior, a parametric sensitivity has been studied. The results of this study show that the higher bearing pressure and lower settlement were achieved when number of geocell layer, secant modulus of geocell and the modulus number of the soil were increased. These results are in-line with the experimental results of the previous researchers. The study also permits the limits of effective and efficient reinforcement to be determined.

KEYWORDS: *Geosynthetic, analytical method, geocell layers, elastic modulus, bearing pressure, settlement*

1. Introduction

In the last decades, due to its cost savings, ease of construction and ability to improve the visual appearance, geosynthetic reinforced soil has been significantly exploited in geotechnical engineering applications such as road construction, railway embankments, lifeline provision, stabilization of slopes, and improvement of soft foundation beds (e.g., Collin et al., 1996; Raymond, 2002; Hufenus et al., 2006; Dash et al., 2007; Bathurst et al., 2009; Madhavi Latha and Somwanshi, 2009a; Zhang et al., 2009; Ling et al., 2009; Palmeira and Andrade, 2010; Pokharel et al., 2010; Boushehrian et al., 2011; Lambert et al., 2011; Yang et al. 2012; Thakur et al., 2012; Tavakoli Mehrjardi et al., 2012; Leshchinsky and Ling, 2013a,b; Yang and Han, 2013; Tanyu et al., 2013, Chen et al., 2013, Soudé et al., 2013; Avesani Neto et al., 2013; Kachi et al., 2013; Moghaddas Tafreshi et al., 2014; Indraratna et al., 2015). A desirable use of such reinforcements would be to improve the bearing capacity and settlement of footings. With this in mind, many researchers have investigated the beneficial ability of planar and cellular reinforcement (e.g. geocell) constructions and how best to arrange the inclusions so as to deliver effective reinforcement and to improve their bearing capacity and settlement response (Dash et al., 2007; Sitharam et al., 2007; Madhavi Latha and Rajagopal, 2007; Zhou and Wen, 2008; Chen and Chiu, 2008; Yoon et al., 2008; Sharma et al., 2009; Wesselo et al., 2009; Sireesh et al., 2009; Eid et al., 2009, Pokharel et al., 2010; Zhang et al., 2010a; Yang et al., 2012; Lambert et al., 2011; Kumar and Kaur, 2012; Tanyu et al., 2013; Tavakoli mehrjardi et al., 2013; Dash and Chandra Bora, 2013; Chen et al., 2013; Mehdipour et al., 2013; Biswas et al., 2013; Hegde and Sitharam, 2014; Huang, 2014, Song et al., 2014).

Recently, two of the current authors have shown that geocell reinforcement can be significantly more effective than a planar reinforcement, in improving the behaviour of foundation beds under static and repeated loads **(**Moghaddas Tafreshi and Dawson**,** 2010a;b**).** They attributed this to the superior confinement offered by the geocells in all directions, due to the frictional and passive resistance developed at the soil-geocell interfaces that increases the sand's bearing capacity and decreases the settlement of the foundation bed.

An analytical approach to the design of such footings and to explain their pressure-settlement behavior would be very useful. Although, there have been many experimental studies into the use of geocell reinforcement in civil engineering works, there are few analytical studies (e.g., Zhang et al. 2009; 2010a;b). Zhang et al. (2010a) presented a simple bearing capacity calculation method for a geocell-supported embankment on a soft subgrade based on the study of the reinforcement functions of a geocell layer beneath a road embankment. They indicated that their results were relatively close to the experimental results. Zhang et al. (2010b) idealized a geocell-reinforced mattress as a beam on a Winkler foundation in order to analyze its settlement response. Semi-analytic

solutions were developed to assess the deformations of, and internal forces in, the foundation 'beam'. They reported that the interface resistance, related to the horizontal deformation of the composite beam (i.e., geocell-soil 'beam'), had a reduction effect on the embankment settlement.

2. Aim

A literature review, briefly reported above, indicated that there remains a lack of analytical study into the behaviour of footings supported by a geocell-reinforced bed, particularly when that bed includes a multi-layered geocell. Therefore, this article seeks to redress this omission by providing a relatively simple analytical method, based on "n"-layered soil system theory (Hirai, 2008) and surface settlement of equivalent system (Vakili et al., 2008), for the evaluation of the pressure-settlement response of both unreinforced and multi-layered geocell-reinforced foundation beds. The results of this method have been compared with the results of plate load tests (Moghaddas Tafreshi et al., 2013) to investigate its validity. In addition, the effects of various parameters such as geocell and soil stiffness modulus, geocell layer height and diameter of plate load have been investigated so as to understand mechanisms for improving the pressure-settlements behaviour of such footings. Note that, although, the settlement-stress behavior of plate loading tests is not elastic, yet the aforementioned analytical method simulated the behavior as a Multiple Linear Elastic (MLE) model (i.e., non-linear elastic) permitting calculation of the elastic modulus of each layer, for each loading step.

3. Problem statement

Geosynthetic inclusions are most effective if used in the zone significantly stressed by the footing. Since, a concentrated stress bowl occupies a zone equal to or twice the depth of the footing width/diameter (the "effective depth" being approximately 1.2 – 2 m for a typical footing width/diameter), and the heights of commercially produced geocells are usually less than 200 mm (available cell depths produced by two key manufacturers in Europe and USA), a single thick layer of geocell beneath the footing is not possible for field construction. Even if it were, such a thick geocell layer would likely make compaction of cell-fill extremely difficult (Thakur et al., 2012; Moghaddas Tafreshi et al., 2014), consequently decreasing the performance of a thick single layer of geocell. Hence, practically, if such a depth of soil needs to be reinforced by geocells, it necessitates designers to use 3 to 4 layers of geocell with thickness $\leq$ 200 mm.

Hence, the use of several layers of geocell (say, three or four) each with a thickness $\leq$ 200mm and with vertical spacing between successive layers of geocell is a practical alternative and could be a beneficial means of reinforcing the soil beneath a footing. The schematic cross-section of the foundation bed containing

geocell-reinforcement layers with the thicknesses of h_g, and of the footing, is shown in Fig. 1. In this figure, the first geocell layer is located at a depth of u beneath the footing and the next geocell layers are placed after an unreinforced soil thickness of h_s. It should be noted that, although there are three probable mechanisms by which geocell transfers stress through the depth of foundation bed ("lateral resistance effect", "vertical stress dispersion effect" and "membrane effect"), this study tried to simulate all these factors by considering soil-geocell layer as a composite material. Some simplification for a complicated problem like the current system is inevitable. Here, the characteristics of the composite material have been defined according to the soil and soil-geocell specimens in triaxial tests; and the simplifying assumptions made in the solution system mean that the behavior of the geocell layers are considered to be uniform layers that only deform vertically. Since the "n"-layered soil system theory by (Hirai, 2008) and surface settlement of equivalent system (Vakili et al., 2008) were employed for the evaluation of the pressure-settlement response of multi-layered geocell-reinforced foundation beds, a summary of these methods is presented in Sections 5 and 6.

4. Pressure-settlement variation of footing on unreinforced bed

For a semi-infinite soil medium of the elastic modulus E_n and Poisson's ratio v_n, subjected to uniform pressure q on a circular footing with radius a, the immediate settlement at the depth z below the center of flexible footing is written as Eq. (1) (Harr, 1966). Eq. (1) is valid for a flexible footing and should be multiplied by $\pi/4$ for a rigid footing.

$$w(z) = \frac{2aq(1-v_n^2)}{E_n}\left(\sqrt{1+\frac{z^2}{a^2}}-\frac{z}{a}\right)\left\{1+\frac{z/a}{2(1-v_n)\sqrt{1+\frac{z^2}{a^2}}}\right\} \quad (1)$$

5. N-Layered Soil System Theory (Hirai, 2008)

Hirai (2008) developed the elastic relationships of multilayer soil stiffness modulus that have been investigated, previously, by Palmer and Barber (1940) and Odemark (1949). Fig. 2 shows a multi-layered soil system composed of n-layers of soil subjected to vertical loads q. As shown in Fig. 2, the present procedure uses the elastic moduli, i.e. Young's modulus of E_m, Poisson's ratio of v_m and thickness of H_m for m^{th} layer in n-layers of multi-layered soil system. Parameters D and D_f are diameter and embedment depth of a footing, respectively.

The n-layered soil system shown in Fig. 2 was transformed into an equivalent two-layered soil system illustrated in Fig. 3a. The equivalent elastic modulus of E_H (Hirai and Kamei, 2003; 2004) for $(n-1)$ layers in Fig. 3a (where $H=H_1+H_2+H_3+\ldots.+H_{n-1}$) was represented by:

$$E_H = \left[\left\{ E_1 \frac{(1-\nu_n^2)}{(1-\nu_1^2)} \right\}^{\frac{1}{3}} \frac{H_1 - D_f}{H - D_f} + \sum_{j=2}^{n-1} \left\{ E_j \frac{(1-\nu_n^2}{(1-\nu_j^2)} \right\}^{\frac{1}{3}} \frac{H_j}{H - D_f} \right]^3 \quad (2)$$

Next, the two-layered soil system in Fig. 3a was transformed into an equivalent single soil layer with elastic modulus of E_n and Poisson's ratio of ν_n, (the thickness of an equivalent single layer is $H=H_e+H_n$) as shown in Fig. 3b, using the equivalent thickness relations (3) and (4) (Hirai and Kamei, 2003; 2004; Hirai, 2008). For the case where $E_H \geq E_n$:

$$H_e - D_f = \left(\frac{E_H}{E_n} \right)^{1/3} (H - D_f) \quad (3)$$

and for the case where $E_H \leq E_n$:

$$H_e - D_f = \left[0.75 + 0.25 \left(\frac{E_H}{E_n} \right)^{1/3} \right] (H - D_f) \quad (4)$$

Likewise, Fig. 4 shows an equivalent system of soil layers to that previously illustrated in Fig. 2, but now each soil layer has an equivalent thickness of H_{ie} and uniform E and ν values for every layer ($=E_n$ and ν_n). Thus the system is reduced to a single layer system of thickness $H_{1e}+H_{2e}+H_{3e}+\ldots.+H_{(n-1)e}+H_n$ and stiffness properties E_n and ν_n. The equivalent thickness of each individual layer is required so as to obtain the thinning and strain of each layer of the multilayered system as described in Section 7.2. According to the Palmer and Barber method (1940) for a two-layer system and to Odemark's method (1949) for a multi-layered soil system, Eqs. (5a) and (5b), respectively, were derived by Hirai (2008) for estimating the equivalent thickness of each layer for the case where $E_m \geq E_n$:

$$H_{1e} - D_f = \left\{ \frac{E_1(1-\nu_n^2)}{E_n(1-\nu_1^2)} \right\}^{1/3} (H_1 - D_f) \quad (5a)$$

$$H_{me} = \left\{ \frac{E_m(1-\nu_n^2)}{E_n(1-\nu_m^2)} \right\}^{1/3} H_m \quad (m = 2 \sim n) \quad (5b)$$

For the case where $E_m \leq E_n$, by considering Terzaghi's approximate formula (1943), the equivalent thickness is given by Eqs. (6a) and (6b):

$$H_{1e} - D_f = \left[0.75 + 0.25\left\{\frac{E_1(1-\nu_n^2)}{E_n(1-\nu_1^2)}\right\}^{1/3}\right](H_1 - D_f) \tag{6a}$$

$$H_{me} = \left[0.75 + 0.25\left\{\frac{E_m(1-\nu_n^2)}{E_n(1-\nu_m^2)}\right\}^{1/3}\right]H_m \quad (m = 2 \sim n) \tag{6b}$$

where H_{1e} and H_{me} are the values of H_e for the first and subsequent layers (m=2 to n), respectively and E_1, ν_1, E_n, ν_n and E_m, ν_m are values of E_H and ν for layers 1, n and m=2 to n, respectively.

6. Surface Settlement of Equivalent System (Vakili et al., 2008)

Vakili et al. (2008) developed the method of Foster and Ahlvin (1959) to evaluate the surface settlement of the equivalent system shown in Fig. 4. According to this method, the actual vertical surface deflection of a footing (w) was obtained by adding the amount of thinning, w_2, of the equivalent layer (with thickness of H_e) between the surface (z=0) and a depth of z=H_e to the vertical deflection at a depth of z=H_e of a semi-infinite mass below that depth (i.e. deflection of w_1 at bottom of the equivalent layer). In the case of uniform pressure "q" on a flexible circular footing with radius "a" (Fig. 4), supported by a semi-infinite mass, w_1 is obtained by substituting the value of z=H_e from Eq. (3)/ or Eq. (4) into Eq. (1) to obtain Eq. (7):

$$w_1 = \frac{2aq(1-\upsilon_n^2)}{E_n}\left(\sqrt{1+\left(\frac{H_e}{a}\right)^2} - \frac{H_e}{a}\right)\left(1 + \frac{H_e}{2a(1-\upsilon_n)\sqrt{1+\left(\frac{H_e}{a}\right)^2}}\right) \tag{7}$$

Similarly, the vertical deflection at the center of loading on surface (i.e. w_0 at depth of z=0) of uniform equivalent layer (i.e. for the footing on the equivalent layer), substituting the value of z=0 into Eq. (1) results:

$$w_0 = \frac{2a(1-\upsilon_n^2)q}{E_n} \tag{8}$$

Eqs. (7) and (8) are valid for a flexible footing and should be multiplied by π/4 for a rigid footing. The vertical thinning of the equivalent layer (with thickness of H_e as in Fig 3b) between the loading surface (z=0) and a depth of $z=H_e$ (i.e. (w_0-w_1)), can be converted to the thinning, w_2, of the original layer (thickness H as in Figs. 2 and 3a), using Eq. (9):

$$w_2 = \frac{E_n}{E_H}(w_0 - w_1) \tag{9}$$

Hence, Eqs. (7) and (9) may be summed to obtain the actual total surface settlement of the circular footing ($w=w_1+w_2$).

7. Pressure-settlement variation of footing on multi-layer geocell-reinforced bed

7.1. Methodology

Fig. 5 shows a schematic model of a shallow circular footing with diameter, $D=2a$, located on a typical n-layer foundation bed composed of "m" geocell layers and "n-m" soil layers, under the application of a uniformly distributed surface load, q. The thicknesses of geocell and soil layers are h_g and h_s, respectively. The first geocell layer is placed at a depth of u beneath the footing and the remaining geocell layers are located after an unreinforced soil thickness of h_s. The effective depth, H_{eff}, is assumed as the depth to a point below the footing at which only 10% of the applied stress on footing surface acts. The elastic modulus, E_i, and Poisson's ratio, v_i (i=1, 2, 3, …., n) of each layer is as given in Fig. 5. H_{n-1} is the thickness of the $(n\text{-}1)^{th}$ layer which can be calculated using Eq. (10).

$$H_{n-1} = H_{eff} - u - mh_g - (m-1)h_s \tag{10}$$

The following simplifying assumptions are made in this analysis, as follows:

- The soil layers are homogeneous, isotropic and non-cohesive;
- The unreinforced and reinforced layers deform only in the vertical direction;
- The footing is circular with no embedment depth, D_f=0;
- The behaviour of unreinforced and reinforced layers is assumed to be nonlinear elastic;
- Poisson's Ratio is assumed to be in the range 0.2 - 0.3 (see below).

Note that, although 'toothpaste' lateral squeezing of soil between geosynthetically-reinforced soil layers is a possibility for plastic soils, granular soils are unlikely to experience this if the reinforcing layers confine the granular soil closely. As observed in the tests at near full-scale by Wu et al. (2013), it is then the reinforcement with the granular soil that controls, partly horizontal movement due to the frictional resistance developed between the reinforcement and the soil and due to the nearby position of the reinforcing layers disrupting potential shear planes/dislocation zones.

However, it is known that geocell layers don't expand much horizontally once properly filled with granular soil and compacted (Dash et al., 2007; Pokharel, 2010). Thus the proposed analytical model does not directly consider lateral deformation but, instead, allows for some, indirectly, by using:

(1) elasticity moduli of the soil and geocell-reinforced layers that were obtained from calibration of the proposed equations (see Section 8.1) to the data obtained in the triaxial test that included some lateral deformation, and

2) Poisson's Ratio values of 0.2 – 0.3, for the unreinforced and geocell-reinforced layers of the foundation bed to compute the equivalent thickness of the multi-layered system (see Section 5), being in-line with typical values as used by Mhaiskar and Mandal (1996) and Zhang et al. (2010c), as described later (see Section 8.1.2).

7.2. Incremental Formulation using Nonlinear Elastic Method

As mentioned in section 2, the "n"-layered soil system theory (Hirai, 2008) and surface settlement of equivalent system (Vakili et al., 2008) were employed to evaluate the pressure-settlement of footings supported by a multi-layer geocell-reinforced bed as shown in Fig. 5. Fig. 3 shows the process of substituting the n-layer system with an equivalent single-layer system, here with the limitation that D_f=0. To do so, firstly, the upper "n-1" layers of thicknesses H_1, H_2, H_3, ….and H_{n-1} (Fig. 5) should be replaced by a single layer of thickness (H_{eff}=H_1+H_2+H_3+….+ H_{n-1}) having an equivalent modulus of E_H in Fig. 6a (Hirai, 2008). The equivalent elastic modulus (E_H) of layers 1 to *n*-1, is calculated by using Eq. (2) for the footing with no embedment depth (D_f=0) as Eq. (11).

$$E_H = \left[\sum_{j=1}^{n-1} \left\{ E_i \frac{(1-\nu_n^2)}{(1-\nu_j^2)} \right\}^{\frac{1}{3}} \frac{H_j}{H_{eff.}} \right]^3 \quad (11)$$

where, H_i and E_i are the thickness and elastic modulus of ith layer, respectively. The *n*-layer system in Fig. 5 is thus reduced to a two layers system as shown in Fig. 6a.

The two-layered system (Fig. 6a) can be reduced to an equivalent single-layer system (Fig. 6b) with elastic modulus of E_n and an equivalent thickness of H_e. The equivalent thickness (H_e) with the elastic modulus of E_n and Poisson's Ratio of ν_n is then defined by Eq. (12a) for the case where $E_H \geq E_n$ and by Eq. (12b) for the case where $E_H \leq E_n$. Eq. (12a) and Eq. (12b) provided for the same Poisson's Ratio of the two layers in Fig. 6a where E_n is the elastic modulus of the nth layer.

$$H_e = \left(\frac{E_H}{E_n} \right)^{1/3} H_{eff} \quad (12a)$$

$$H_e = \left[0.75 + 0.25 \left(\frac{E_H}{E_n} \right)^{1/3} \right] H_{eff} \quad (12b)$$

Consequently, the use of Eq. (11) and Eq. (12) deliver an equivalent single homogeneous semi-infinite mass of material which can be substituted for the *n*-layer system as shown in Fig. 6b.

Generally, the footing settlement (i.e, soil surface settlement), *w* should be calculated using Eqs. (7) to (10). Since, the nature of footing pressure-settlement variation is nonlinear, the behavior of unreinforced layers and reinforced layers (Geocell and soil inside of its pockets) are considered to act as MLE (Multiple Linear Elastic) layers. The MLE model provides an ability to calculate the elastic modulus of each layer, for each load step, using the confining pressure of the current and previous stages as described in Eqs. (13) to (23).

To calculate the elastic modulus of the i^{th} layer, requires knowledge of the strain of layers 1 to *n*-1. To compute these, the deformation and equivalent thickness of the i^{th} layer (Fig. 5) are required. Using Eq. (5) and Eq. (6) for the footing with no embedment depth (D_f=0), supported on a multi-layer system, the

equivalent thickness of each soil layer, H_{ie} with the same E_n and v_n was determined by Eq. (13a) for the case where $E_i \geq E_n$ and by Eq. (13b) for the case where $E_i \leq E_n$, respectively.

$$H_{ie} = \left\{ \frac{E_i (1-\nu_n^2)}{E_n (1-\nu_i^2)} \right\}^{1/3} H_i \tag{13a}$$

$$H_{ie} = \left[0.75 + 0.25 \left\{ \frac{E_i (1-\nu_n^2)}{E_n (1-\nu_i^2)} \right\}^{1/3} \right] H_i \tag{13b}$$

Then, from Eqs. (7) and (9), for a rigid circular footing with radius a subjected to uniform pressure q, the thinning and strain of the i^{th} layer are defined as Eqs. (14) to (16):

$$w_i = \frac{2\pi a q (1-\upsilon_n^2)}{4E_n} \left(\sqrt{1+\left(\frac{\sum_{l=1}^{l=i} H_{le}}{a}\right)^2} - \frac{\sum_{l=1}^{l=i} H_{le}}{a} \right) \left(1 + \frac{\sum_{l=1}^{l=i} H_{le}}{2a(1-\upsilon_n)\sqrt{1+\left(\frac{\sum_{l=1}^{l=i} H_{le}}{a}\right)^2}} \right) \tag{14}$$

$$w_{p_i} = \frac{E_n}{E_i} \left(w_i - w_{i-1} \right) \tag{15}$$

$$\varepsilon_i = \frac{w_{p_i}}{H_i} \tag{16}$$

Where:

H_{ie}: equivalent thickness of the ith layer based on the elastic parameters of the n^{th} layer

w_i: displacement at a depth of $\sum_{l=1}^{l=i} H_{le}$

w_{pi}: the vertical deformation within the i^{th} layer of thickness H_{ie},(due to actual thinning of the i^{th} layer)

ε_i: the strain across the thickness of the i^{th} layer

In the j^{th} loading step, the displacement increment of soil surface due to loading increment of q_j-q_{j-1} can be calculated by Eqs. (17) to (20):

$$\Delta w_1^j = \frac{2\pi a(q_j - q_{j-1})(1-\upsilon_n^2)}{4E_n}\left(\sqrt{1+\left(\frac{H_e}{a}\right)^2} - \frac{H_e}{a}\right)\left(1+\frac{H_e}{2a(1-\upsilon_n)\sqrt{1+\left(\frac{H_e}{a}\right)^2}}\right) \quad (17)$$

$$\Delta w_0^j = \frac{2\pi a(1-\upsilon_n^2)(q_j - q_{j-1})}{4E_n} \quad (18)$$

$$\Delta w_2^j = \frac{E_n}{E_H}\left(\Delta w_0^j - \Delta w_1^j\right) \quad (19)$$

$$w^j = w^{j-1} + \Delta w_1{}^j + \Delta w_2{}^j \quad (20)$$

Where:

Δw_1^j : vertical displacement increment on loading centerline at a depth of H_e for loading increment of q_j-q_{j-1}, (i.e. at the bottom of the equivalenced layer)

Δw_0^j : vertical displacement increment at surface (of equivalent layer) beneath centre of load for loading increment of q_j-q_{j-1},

Δw_2^j : vertical deformation (thinning) increment of the original layer of thickness of H,

w^j : vertical displacement at surface of system for loading of q_j.

Similarly, the strain increment for the i^{th} layer at the j^{th} loading step can be calculated using Eqs. (21) to (23) using the adjustments already employed to formulate Eqs. (14) and (16):

$$\Delta w_i^j = \frac{2\pi a(q_j - q_{j-1})(1-\upsilon_n^2)}{4E_n}\left(\sqrt{1+\left(\frac{\sum_{l=1}^{l=i} H_{le}}{a}\right)^2} - \frac{\sum_{l=1}^{l=i} H_{le}}{a}\right)\left(1+\frac{\sum_{l=1}^{l=i} H_{le}}{2a(1-\upsilon_n)\sqrt{1+\left(\frac{\sum_{l=1}^{l=i} H_{le}}{a}\right)^2}}\right) \quad (21)$$

$$(\Delta w_p)_i^j = \frac{E_n}{E_i}\left(\Delta w_i^j - \Delta w_{i-1}^j\right) \quad (22)$$

$$\varepsilon_i^j = \varepsilon_i^{j-1} + \frac{(\Delta w_p)_i^j}{H_i} \quad (23)$$

where:

H_{ie}: equivalent thickness of the i^{th} layer based on the elastic parameters and thickness of the n^{th} layer as defined by Eq (13),

Δw_i^j : displacement increment of equivalent layer for layers 1 to i based on the elastic parameters of n^{th} layer in depth of $\sum_{l=1}^{l=i} H_{le}$ for loading increment of q_j-q_{j-1},

$(\Delta w_p)_i^j$: deformation increment (thinning) of layer with thickness of H_i for loading increment q_j-q_{j-1},

ε_i^j : strain of layer with thickness of H_i subjected to loading q_j.

8. Results and discussion

To validate the results of the method presented above, the pressure-settlement response of a footing on unreinforced and geocell-reinforced beds was estimated and compared with the results of four static plate load tests (Moghaddas Tafreshi et al., 2013). As Fig. 7 shows, they performed the static plate load tests of a footing supported on unreinforced soil and reinforced soil with geocell layers in a test pit measuring 2000×2000 mm in plane and 700 mm in depth using a 300 mm diameter rigid plate. The vertical distances of the first layer of geocell (u) from the footing and also that from each other (h_s) were 0.2 times the footing diameter. Also, the width of the geocell layers (b) was held constant at 5 times the footing diameter ($b/D=5$). Since the horizontal dimensions of the test pit were about seven times bigger than the diameter of the footing model and it was observed that the soil surface bulging around the footing model extended less than 1.5 times the footing diameter from the circumference of the footing, the boundary effect of the pit walls on the test results was likely insignificant. Also, regarding the test pit depth, the zone of influence of the footing will be over a depth of less than 2 diameters beneath the footing (the "effective depth"), so the boundary effect of test pit base on the test results may also be considered to be insignificant. Thus it should be viable to compare the analysis results with the experimental ones.

The soil was well graded sand (SW, according to the Unified Soil Classification System, ASTM D 2487-11) with a specific gravity of 2.68 and passing through the 38 mm sieve. The geocell used in the tests was non-perforated and fabricated from continuous polypropylene filaments as a non-woven geotextile, with

ultimate tensile strength of 13.1 kN/m and pocket size of 110×110×100 mm^3 (lenght×width×height). The details of engineering properties of the geotextile and soil properties are given by Moghaddas Tafreshi et al., (2013).

As part of this validation, the effects of several parameters including geocell and soil stiffness modulus, geocell layer height and number of geocell layers on pressure-settlement response of footing were investigated. The results of triaxial tests on unreinforced and geocell reinforced soil samples were used to estimate the elastic modulus of the different layers during the loading steps (Noori, 2012). The soil, geocell material and the density of the soil filled into the geocell pockets, used in both the plate load tests and triaxial tests were the same. Six triaxial tests on unreinforced and reinforced soil samples with one layer of geocell, at three confining pressures of 50, 100 and 150 kPa were conducted. The triaxial samples had a diameter of 100 mm and a height of 200 mm as shown in Fig. 8. The geocell-soil composites layers are of 100 mm in diameter and 100 mm in height and positioned at mid-height of the specimen. The stress-strain response of unreinforced and geocell reinforced samples with single layer of the geocel-soil composite under three confining pressures are shown in Fig. 9. This figure indicates that the geocell reinforcement increases the deviator stress (i.e., shear strength) of the samples considerably compared to unreinforced samples, irrespective of confining pressure. This behavior is essentially due to the increase in confining effect of geocell layers which cause an internal confinement in reinforced samples. On the other hand, vertical stress applied to the infill induces a horizontal active pressure at the perimeter of the cell of geocell. The infill wall interface friction transfers load into the cell structure which, in turn, mobilises resistance in surrounding cells. It is also evident that cells that surround a loaded cell offer greater passive resistance due to the lateral strain in the vicinity of the load– consequently leading to an improvement in the overall performance in strength.

Note that, triaxial compression tests on a single geocell layer sandwiched between two soil layers may give different results compared to the test on a single, less constrained geocell. Since, the present analytical formulation was employed to simulate the results of plate load tests supported by geocell layers of 100 mm thickness, thus using a single layer of geocell with the same thickness in triaxial test sample with a height of 200 mm was inevitable.

8.1. Elastic modulus of unreinforced and geocell-reinforced layers

Since the six triaxial tests were conducted at three specified confining pressures of 50, 100 and 150 kPa, thus the tangential elastic modulus at different strain levels can be obtained from the stress-strain responses in Fig. 9,

when the confining pressures are exactly 50, 100, and 150 kPa. Hence, at each stage of loading during the analysis, a continuous function of confining pressure and axial strain is required to obtain the tangential elastic modulus when the strain level and confining pressure being varied. Thus, in this section the elastic modulus of unreinforced and geocell-reinforced soil layers in terms of strain and confining pressure, $E=f(\sigma_3,\varepsilon)$ for each loading step, was modeled non-linearly from the data of six triaxial tests at the three confining pressures of 50, 100 and 150 kPa (see Fig. 9).

8.1.1. Elastic modulus of unreinforced layers

Based on the data extracted from Fig. 9a, the vertical stress ($\sigma_1=\sigma_3+\sigma_d$) of triaxial samples was found to be a function of the confining pressure (σ_3) and axial strain (ε). Therefore a nonlinear regression model was developed to estimate the vertical stress (σ_1) for different values of σ_3 and ε.

Several alternative modeling approaches were trialed before selecting, as optima, a non-linear power model with of the largest multiple coefficient of determination, R^2=0.91, and a minimum value of standard error, E_s=0.11, to estimate the vertical stress (σ_1) as a function of different parameters was obtained as Eq. (24):

$$\sigma_1 = 61.47\ \sigma_3^{0.73}\ \varepsilon^{0.34}\ e^{-3.17\varepsilon} \tag{24}$$

Using Eq. (24), the absolute average percentage of error, e_{ave} and maximum percentage of error, e_{max} in estimating the value of σ_1 were found to be 2.5% and 4.6% respectively.

The tangential modulus of elasticity can be derived as the derivative of stress with respect to strain (from Eq. (24)) as presented in Eq. (25a). The function of f (ε) is defined in Eq. (25b).

$$E = 61.47\ \sigma_3^{0.73} * f\ (\varepsilon) \tag{25a}$$

$$f\ (\varepsilon) = (-3.17\ e^{-3.17\varepsilon}\varepsilon^{0.34} + \frac{0.34\ \varepsilon^{0.34}}{\varepsilon} e^{-3.17\varepsilon}) \tag{25b}$$

8.1.2. Elastic modulus of geocell-reinforced layers

Madhavi Latha (2000), based on the results of triaxial compression tests on geocell-encased sand, proposed an empirical equation in the form of Eq. (26) to express the elastic modulus of the geocell reinforced sand (E_g).

$$E_g = 4\ \sigma_3^{0.7}(K_u\ + 200M^{0.16}) \tag{26}$$

Where:

K_u: the dimensionless modulus number of the unreinforced sand in the hyperbolic model proposed by Duncan and Chang (1970),

M: the secant tensile modulus of the geocell material (e.g., geotextile and geogrid) in *kN/m*, assessed at an average strain of 2.5% in load-elongation, and

σ_3: the confining pressure in kPa.

In fact, the geocell layers are modeled as equivalent composite layers with enhanced stiffness and shear strength properties. The term in parentheses of Eq. (26) expresses the Young's modulus parameter of geocell-reinforced soil in terms of the secant modulus of the geocell material (M) and the dimensionless modulus number of the unreinforced soil (K_u).

However, due to the fact that the suggested relationship by Madhavi Latha (2000), Eq. (26), is not a function of axial strain level, it is modified to Eq. (27) as a function of both confining pressure (σ_3) and axial strain (ε).

$$E_g = a_1 \sigma_3^{b_1} (K_u + a_2 M^{b_2}) * f(\varepsilon) \quad (27)$$

The function of $f(\varepsilon)$ is assumed as Eq. (25b) and then the parameters of a_1, a_2, b_1 and b_2 are obtained from the triaxial tests results of geocell-reinforced soil (Fig. 9b).The constants parameters in Eq. (27) depend on the type of infill soil and strength of geocell material, which must be calibrated according to the results of triaxial tests on soil and geocell, with the same properties that would be used in the foundation bed. Fitting Eq. (27) to the data of Noori (2012) yields the elastic modulus as a function of σ_3, ε, K_u and M as Eq. (28).

$$E_g = 0.12 \sigma_3^{0.73} (K_u + 100 M^{0.1}) * f(\varepsilon) \quad (28)$$

At each loading step, the elastic modulus of unreinforced and reinforced layers were estimated using the confining pressure (at mid-height of the layer) and the strain computed at the end of the previous loading step. The confining pressure in the middle of each reinforced layer was obtained by multiplying the distributed vertical stress by the coefficient of lateral pressure (k_r). The value of k_r is proposed by authors as Eq. (29), in which the value of lateral pressure coefficient for unreinforced soil k_{un}=0.5 has been suggested by Madhavi Latha (2000). For the M=0, Eq. (29) results the lateral pressure coefficient of unreinforced soil (k_{un}).

$$k_r = k_{un} (K_u + 100 M^{0.1}) / K_u \quad (29)$$

Overall, Eqs. (25a) to (29) reveal that the proposed formulations would be able to consider the variation of geocell performance in regard to the strain level and confinement stress variations across the depth of the

foundation bed, provided the elastic modulus of the different layers (soil layers and the geocell-reinforced layers) are allotted appropriate values that differ from layer-to-layer and from one loading step to the next. Based on the results of triaxial compression tests, the value of the hyperbolic parameter of Duncan and Chang (1970), K_u, is found as 483.3 (the authors' evaluation not reported here). Also, the secant modulus of the geocell material at 2.5% strain, M, is given by the manufacturer as 114 kN/m (M= 114 kN/m). Due to the confinement of the soil by the geocell wall, the Poisson's ratio of geocell-reinforced layers may be less than that in unreinforced layers. The range of Poisson's ratio for granular soil (i.e. sand in the present paper) is about 0.3-0.35 and for geocell filled with sand from 0.17 (Mhaiskar and Mandal, 1996) to 0.25 (Zhang et al., 2010c). Thus, a Poisson's ratio of 0.3 is used for unreinforced layers and a Poisson's ratio of 0.25, 0.2, and 0.2, is used respectively for reinforced layers with one, two and three layers of geocell.

8.2. Validation of proposed analytical method

The presented analytical method was validated by comparing the results of model analyses with plate load tests results (Moghaddas Tafreshi et al., 2013) for an unreinforced bed and for beds reinforced by one, two and three layers of geocell. Fig. 10 compares the results of the analytical method and tests in the form of footing pressure-settlement responses, for different values of geocell mass. These comparisons are done for parameters of K_u=483.3, M= 114 kN/m, h_g=100 mm and D=300 mm. Since, the analytical method has not considered any variation in the geocells' width; it is assumed that the width of the geocell-reinforced layers being sufficient to ensure the anchorage derived from the adjacent stable soil mass.

The predicted responses show a better match with the experimental ones at lower footing settlement levels (i.e., s/D<8%). For larger footing settlements (e.g., s/D>8%), the analytical predictions under-estimate the experimentally determined settlements, implying strain softening in the geocell-soil layers in-situ relative to the performance in the triaxial or that the assumption of no lateral strain is non-conservative. The difference between the predicted responses and experimental ones might more generally be attributed to the selected value of lateral pressure coefficient, the selected values of Poisson's ratio, the simplifying assumptions used in the analytical method, the discrepancies between the experimental and analytical systems and the differences in simulating the field and the experimental conditions of multiple layers.

Since the practical design of shallow footings is mostly governed by footing settlement, footing settlement must be limited to specific values, depending on the super-structure. Thus, the close comparison of analytical and experimental results in the lower range of settlement (i.e., less than 6% of the footing

diameter) is encouraging. This implies that the analytical method presented is capable of estimating the behavior of footings supported by geocell layers and may be conveniently applied as a tool to estimate the pressure-settlement response of footings over most practical ranges of geotechnical use.

8.3. Predictive parametric study

Using the analytical model presented, a parametric study was carried out to account for the variability of those parameters that could not be considered in the physical tests, so as to verify the model's predictive capability. Particularly, variation in the secant modulus of geocell (M), the dimensionless modulus number of the soil (K_u), the thickness of geocell layers (h_g) and the number of geocell layers (N_g) were investigated in this way.

Fig. 11a shows the effect of the secant modulus of the geocell (M) on the pressure-settlement response of a foundation reinforced with three layers of geocell. The results reveal the beneficial effect of the reinforcement's rigidity (see Eq. (28)) in decreasing the footing settlements, so that at a given bearing pressure, the value of the settlement decreases as the secant modulus of geocell (M) increases. The similar results reported by Madhavi Latha et al. (2006) for geocell-supported embankments showed that higher surcharge capacity and lower deformations are associated with increase in the value of the M parameter. This performance could be attributed to the internal confinement provided by geocell reinforcement with increase in M. The confinement effect is dependent on the secant modulus of the reinforcement, the friction at the soil-reinforcement interface and the confining stress developed on the infilling soil inside the geocell pocket due to the passive resistance provided by the 3D structure of geocell (Sireesh et al., 2009; Moghaddas Tafreshi and Dawson, 2010a). In addition, as seen in Fig. 11a, there is a limiting value of M (=100 kN/m) beyond which no further load-settlement benefit is achieved. Almost certainly this is because the behavior of the unreinforced soil between the reinforced layers is now limiting the response of the overall system.

To see what the effect of K_u is, the variation of pressure-settlement of the reinforced bed with three layers of geocell is presented in Fig. 11b. The results show that the bearing capacity of a footing at a given settlement is significantly increased due to an increase in the K_u value. Thus, the role of the soil type and the soil compaction in performance of geocell-reinforced beds, which the composite model suggested in the present study, can take into account this effect. However, a dense sand matrix tends to dilate under footing penetration, thereby mobilizing higher strength in the geocell reinforcement, leading to greater performance improvement (Madhavi Latha et al., 2009b).

The rigidity of the geocell layer is predominantly influenced by the thickness of geocell. To have a better assessment of the effect of a geocell's thickness in a geocell-reinforced foundation, the variation of the pressure-settlement relationship of the unreinforced bed and of the reinforced bed with three layers of geocell is presented in Fig. 11c. The benefit of a thicker geocell mat is evident, so that a thicker geocell decreases the footing settlements, tending to improve its bearing capacity. This appears to be a consequence of greater opportunity of geocell-soil interaction (in the form of wall-friction and confining pressure imposed by the pocket walls) and the increased stiffness of the effective zone beneath the footing consequent upon an increase in the thickness of geocell. This is in-line with the findings of Dash et al. (2007), Sitharam et al. (2007), Madhavi Latha et al. (2006) Moghaddas Tafreshi and Dawson (2010a) who reported that the settlement of a trench's soil surface was decreased due to the provision of a thicker geocell in the backfill. Furthermore, the rate of reduction in footing settlement and the rate of enhancement in load carrying capacity of the footing can also be seen to reduce with increase in the value of h_g. The reason is that, as multiple, thicker reinforcement layers are used, then the reinforced zone extends deeper beyond the zone most significantly strained by the applied load, so that little further benefit accrues. From a practical point of view, as the thickness of a geocell layer is increased; the problem of lower achieved compaction in the geocell packets would be encountered, so that higher compactive effort is necessary as the thickness of vertical webs of the geocell is increased, owing to hindering of vertical densification (Thakur et al., 2012; Tavakoli Mehrjardi et al., 2013). For this reason, multiple thin geocell layers may, in practice, be preferred to fewer, thicker layers.

Fig. 11d presents the bearing pressure-settlement response of the unreinforced and reinforced foundation beds with one, two, three layers of geocell. From this figure, it may be clearly observed that, as the number of geocell layers increases (i.e., the increase in the depth of the reinforced zone), both stiffness and bearing pressure at a specified settlement increase substantially. Likewise, at a given bearing pressure, the value of the settlement decreases as the number of geocell layers increases. However, the rate of reduction in footing settlement is seen to reduce with increase in the number of geocell layers. It is likely that the additional layers are interacting with soil that is strained less and less by the applied load, therefore delivering diminishing increments of additional reinforcement effect. Yoon et al. (2008) and Moghaddas Tafreshi et al. (2013) in their studies on the effect of multi-layered geocell reported a similar effect with increase in the number of 3D reinforcement layers.

9. Conclusions

In this study, an analytical approach based on the theory of multi-layered soil system theory (Hirai, 2008; Vakili et al., 2008) was developed to estimate the pressure-settlement response of a circular footing supported by unreinforced and multi-layered reinforced beds. Definition of elastic modulus for unreinforced and reinforced layers in terms of strain and confining pressure, along with the equivalent elastic method were the main processes of problem solution. The new method delivers predictions of load-settlement that are in good agreement with measured values for a geocell-reinforced application, and thus gives confidence of its usefulness for expected geotechnical applications. The results of the new model, as applied to geocell installations, can be summarized as follows:

(1) The response of pressure-settlement in both reinforced and unreinforced conditions is nonlinearly and significantly affected by the secant modulus of geocell, the dimensionless modulus number of the soil, thickness of geocell layers and the number of geocell layers.

(2) The results emphasized that the performance of geocell-reinforced foundation is always much better than when unreinforced.

(3) The analytical results show that the increase in the number of geocell layers, the secant modulus of the geocell and the dimensionless modulus number of the soil, strengthen the behavior of geocell-reinforced foundation against the surface loading, which is in-line with the experimental results of researchers.

(4) The parametric study shows a decrease in rate of enhancement in bearing pressure, at a given footing settlement with increase in the number of geocell layers, the secant modulus and the thickness of geocell layers.

It should be stated that the results obtained are based on a circular loading plate, one type of geocell reinforcement, fixed width of geocell layers and non-cohesive soil. Consequently, specific applications should only be made after considering the above limitations.

References

American Society for Testing and Materials, 2011. Standard practice for classification of soils for engineering purposes (Unified Soil Classification System). ASTM International, West Conshohocken, PA, D 2487-11.

Avesani Neto, J.O., Bueno, B.S., Futai, M.M., 2013. A bearing capacity calculation method for soil reinforced with a geocell. Geosynth. Int. 20 (3), 129 –142.

443 Bathurst, R.J., Nernheim, A., Walters, D.L., Allen, T.M., Burgess, P., Saunders, D.D., 2009. Influence of reinforcement
444 stiffness and compaction on the performance of four geosynthetic – reinforced soil walls. Geosynth. Int. 16 (1), 43–
445 49.

446 Biswas, A., .Murali Krishna, A., Dash, S.K., 2013. Influence of subgrade strength on the performance of geocell-
447 reinforced foundation systems. Geosynth. Int. 20 (6), 376 –388.

448 Boushehrian, A.H., Hataf, N., Ghahramani, A., 2011. Modeling of the cyclic behavior of shallow foundations resting on
449 geomesh and grid-anchor reinforced sand. Geotext. Geomembr. 29 (3), 242-248.

450 Chen, R.H., Chiu, Y.M., 2008. Model tests of geocell retaining structures. Geotext. Geomembr. 26 (1), 56-70.

451 Chen, R.H., Huang, Y.W., Huang, F.C., 2013. Confinement effect of geocells on sand samples under triaxial
452 compression. Geotext. Geomembr. 37 (2), 35-44.

453 Chen, R.H., Wu, C.P., Huang, F.C., Shen, C.W., 2013. Numerical analysis of geocell-reinforced retaining structures.
454 Geotext. Geomembr. 39 (4), 51-62.

455 Collin, J.G., Kinney, T.C., Fu, X., 1996. Full scale highway load test of flexible pavement systems with geogrid
456 reinforced base courses. Geosynth. Int. 3 (4), 537–549.

457 Dash, S.K., Rajagopal, K., Krishnaswamy, N.R., 2007. Behaviour of geocell reinforced sand beds under strip loading.
458 Can. Geotech. J. 44 (7), 905–916.

459 Dash, S.K., Chandra Bora, M., 2013. Improved performance of soft clay foundations using stone columns and geocell-
460 sand mattress. Geotext. Geomembr. 41 (November), 26-35.

461 Duncan, J. M., Chang, C. Y., 1970. Nonlinear analysis of stress and strain in soils. J. Soil Mech. and Found. 96 (5),
462 1629–1653.

463 Foster, C. R., Ahlvin, R. G., 1959. Stresses and deflections induced by a uniform circular load, Proc. Highway Research
464 Board. 33, 467-470.

465 Harr, M.E., 1966. Foundations of theoretical soil mechanics. McGraw-Hill: New York.

466 Hegde, A., Sitharam, T.G., 2015. 3-Dimensional numerical modelling of geocell reinforced sand beds. Geotext,
467 Geomembr. 43 (2), 171–181.

Hegde, A., Sitharam, T.G., 2015. 3-Dimensional numerical analysis of geocell reinforced soft clay beds by considering the actual geometry of geocell pockets. Can. Geotech. J. Published on the web 14 February 2015, 10.1139/cgj-2014-0387.

Hirai, H., Kamei, T.A., 2003. A method to calculate settlement, stress and allowable stress of multi-layered ground. J.of Struct. Constr. Eng. 573, 81–88.

Hirai, H., Kamei, T., 2004. A method to calculate settlement, stress, failure and allowable stress of multi-layered ground by equivalent thickness theory. J. of Struct. Constr. Eng. 581, 79–86.

Hirai, H., 2008. Settlements and stresses of multi-layered grounds and improved grounds by equivalent elastic method. International. J. for Num. Analy. Meth. Geomech. 32 (5), 523–557.

Eid, H.T., Alansari, O.A., Odeh, A.M., Nasr, M.N., Sadek, H.A., 2009. Comparative study on the behavior of square foundations resting on confined sand. Can. Geotech. J. 46 (4), 438-453.

Huang, C.C., 2014. Force equilibrium-based finite displacement analyses for reinforced slopes: Formulation and verification. Geotext. Geomembr. 42 (4), 394-404.

Hufenus, R., Rueegger, R., Banjac, R., Mayor, P., Springman, S.M., Bronnimann, R., 2006. Full-scale field tests on geosynthetic reinforced unpaved on soft subgrade. Geotext. Geomembr. 24 (1), 21–37.

Indraratna, B., Biabani, M., Nimbalkar, S., 2015. Behavior of Geocell-Reinforced Subballast Subjected to Cyclic Loading in Plane-Strain Condition. J. Geotech. Geoenviron. Eng. 141 (1), 10.1061/ (ASCE) GT.1943-5606.0001199.

Kachi, T.,Kobayashi, M., Seki, M., Koseki, J., 2013. Reinforcement of railway ballasted track with geosynthetic bags for preventing derailment. Geosynth. Int. 20 (5), 316 –331.

Kumar, A., Kaur, A., 2012. Model tests of square footing resting on fibre-reinforced sand bed. Geosynth. Int. 19 (5), 385-392.

Lambert, S., Nicot, F.,Gotteland, P., 2011. Uniaxial compressive behavior of scrapped tire and sand-filled wire netted geocell with a geotextile envelope. Geotext, Geomembr. 29 (5), 483-490.

Leshchinsky, B., Ling, H., 2013a. Numerical modeling of behavior of railway ballasted structure with geocell confinement. Geotext. Geomembr. 36 (1), 33–43.

Leshchinsky, B., Ling, H., 2013b. Effects of Geocell Confinement on Strength and Deformation Behavior of Gravel. J. Geotech. Geoenviron. Eng. 139 (2), 340-352.

Ling, H., Leshchinsky, D., Wang, J.P., Mohri, Y., Rosen, A., 2009. Seismic Response of Geocell Retaining Walls: Experimental Studies. J. Geotech. Geoenviron. Eng. 135 (4), 515-524.

Madhavi Latha, G.M., 2000. Investigation on the behavior of geocell supported embankments. Ph.D. Thesis, Department of Civil Engineering, Indian Institue of Technology Madras, Chennai.

Madhavi Latha, G.M., Rajagopal, K., Krishnaswamy, N. R., 2006. Experimental and theoretical investigations on geocell-supported embankments. Int. J. of Geomech. ASCE, 6 (1), 30–35.

Madhavi Latha, G.M., Rajagopal, K. 2007. Parametric finite element analyses of geocell supported embankments. Can. Geotech. J. 44 (8), 917-927.

Madhavi Latha, G.M., Somwanshi, A., 2009a. Bearing capacity of square footings on geosynthetic reinforced sand. Geotext. Geomembr. 27 (4), 281–294.

Madhavi Latha, G.M., Dash, S. K., Rajagopal, K., 2009b. Numerical simulation of the behavior of geocell reinforced. Int. J. of Geomech. ASCE, 9 (4), 143–152.

Mehdipour, I., Ghazavi, M., Ziaie Moayed, R., 2013. Numerical study on stability analysis of geocell reinforced slopes by considering the bending effect. Geotext. Geomembr. 37 (April), 23-34.

Mhaiskar, S.Y., Mandal, J.N., 1996. Investigations on soft clay subgrade strengthening using geocells. Construc. Build. Mater. 10 (4), 281–286.

Moghaddas Tafreshi, S.N., Dawson, A.R., 2010a. Comparison of bearing capacity of a strip footing on sand with geocell and with planar forms of geotextile reinforcement. Geotext. Geomembr. 28 (1), 72–84.

Moghaddas Tafreshi, S.N., Dawson, A.R. 2010b. Behaviour of footings on reinforced sand subjected to repeated loading – Comparing use of 3D and planar geotextile. Geotext. Geomembr. 28 (5), 434–447.

Moghaddas Tafreshi, S.N., Khalaj, O., Dawson, A.R., 2013. Pilot-scale load tests of a combined multi-layered geocell and rubber-reinforced foundation. Geosynth. Int. 20 (3), 143–161.

Moghaddas Tafreshi, S.N., Khalaj, O., Dawson, A.R., 2014. Repeated loading of soil containing granulated rubber and multiple geocell layers. Geotext. Geomembr. 42 (1), 25-38.

Noori, B., 2012. Experimental investigation of the behavior of geocell reinforced rubber-soil mixture, Msc thesis, Faculty of Civil Engineering, K.N. Toosi University of Technology, Tehran, Iran.

521 Odemark, N., 1949. Investigations as to the elastic properties of soils and design of pavements according to the theory of
522 elasticity. Statens Vaginstitute: Meddelande, Stockholm, Sweden, vol. 77.

523 Palmeira, E.M., Andrade, H.K.P.A., 2010. Protection of buried pipes against accidental damage using geosynthetics.
524 Geosynth. Int. 17 (4), 228–241.

525 Palmer, L.A., Barber, E.S., 1940. Soil displacement under a circular loaded area. Proceedings of the Highway Research
526 Board, 20, 279–286.

527 Pokharel, S. K., Han, J., Leshchinsky, D., Parsons, R. L., Halahmi, I., 2010. Investigation of factors influencing behavior
528 of single geocell-reinforced bases under static loading. Geotext. Geomembr. 28 (6), 570-578.

529 Pokharel, S. K., 2010. Experimental Study on Geocell-Reinforced Bases under Static and Dynamic Loading, PhD thesis,
530 Univ. Kansas, USA.

531 Raymond, G.P., 2002. Reinforced ballast behaviour subjected to repeated load. Geotext. Geomembr. 20 (9), 39-61.

532 Sharma, R., Chen, Q., Abu-Farsakh, M., Yoon, S., 2009. Analytical modeling of geogrid reinforced soil foundation.
533 Geotext. Geomembr. 27 (1), 63–72.

534 Sireesh, S., Sitharam, T.G., Dash, S.K., 2009. Bearing capacity of circular footing on geocell–sand mattress overlying
535 clay bed with void. Geotext. Geomembr. 27 (2), 89–98.

536 Sitharam, T.G., Sireesh, S., Dash, S.K., 2007. Performance of surface footing on geocell-reinforced soft clay beds.
537 Geotech. Geolo. Eng. 25 (5), 509–524.

538 Song, F., Xie, Y.L., Yang, Y.F., Yang, X.H., 2014. Analysis of failure of flexible geocell-reinforced retaining walls. in
539 the centrifuge. Geosynth. Int. 21(6,) 342 –351.

540 Soudé, M., Chevalier, B., Grédiac, M., Talon, A., Gourvès, R., 2013. Experimental and numerical investigation of the
541 response of geocell-reinforced walls to horizontal localized impact. Geotext. Geomembr. 39 (August), 39-50.

542 Tanyu, B.F., Aydilek, A.H., Lau, A.W., Edil, T.B., Benson, C.H. 2013. Laboratory evaluation of geocell-reinforced
543 gravel subbase over poor subgrades. Geosynth. Int. 20 (2), 47 –61.

544 Tavakoli Mehrjardi, Gh., Moghaddas Tafreshi, S.N., Dawson, A.R., 2012. Combined use of geocell reinforcement and
545 rubber–soil mixtures to improve performance of buried pipes. Geotext. Geomembr. 34 (October), 116-130.

546 Tavakoli Mehrjardi, Gh., Moghaddas Tafreshi, S. N., Dawson, A. R., 2013. Pipe response in a geocell reinforced trench
547 and compaction considerations. Geosynth. Int. 20 (2), 105-118.

548 Terzaghi K. Theoretical Soil Mechanics. Wiley: New York, 1943.

549 Thakur, J.K., Han, J., Pokharel, S.K., Parsons, R.L., 2012. Performance of geocell-reinforced recycled asphalt pavement
550 (RAP) bases over weak subgrade under cyclic plate loading. Geotext. Geomembr. 35 (December), 14-24.

551 Yang, X., Han, J., Pokharel, S.K., Manandhar, C., Parsons, R.L., Leshchinsky, D., Halahmi, I., 2012. Accelerated
552 pavement testing of unpaved roads with geocell-reinforced sand bases. Geotext. Geomembr. 32, (June), 95-103.

553 Yang, X., Han, J., 2013. Analytical Model for Resilient Modulus and Permanent Deformation of Geosynthetic-
554 Reinforced Unbound Granular Material. . J. Geotech. Geoenviron. Eng. 139 (9), 1443-1453.

555 Yoon, Y. W., Heo, S. B., Kim, S. K., 2008. Geotechnical performance of waste tires for soil reinforcement from chamber
556 tests. Geotext. Geomembr. 26 (1), 100-107.

557 Vakili Ninyo, J., Moore, I., 2008. A simplified method for evaluation of pavement layers moduli using surface deflection
558 data. The 12th International Conference of International Association for Computer Methods and Advances in
559 Geomechanics (IACMAG), Goa India, 1-6.

560 Wesselo, J., Visser, A.T., Rust, E., 2009. The stress–strain behaviour of multiple cell geocell packs. Geotext. Geomembr.
561 27 (1), 31-38.

562 Wu, J.T.H., Pham, T.Q. Adams, M.T., 2013. Composite Behavior of Geosynthetic Reinforced Soil Mass. Denver, Co.,
563 University of Colorado Denver, Dept. of Civil Engineering ; McLean, VA : Federal Highway Administration, Office
564 of Infrastructure Research and Development, 2013-07 (FHWA-HRT-10-077), 214 pp.

565 Zhang, L., Zhao, M., Zou, X., Zhao, H. 2009. Deformation analysis of geocell reinforcement using Winkler model.
566 Comput. Geotech. 36 (6), 977-983.

567 Zhang, L., Zhao, M., Shi, C., Zhao, H., 2010a. Bearing capacity of geocell reinforcement in embankment engineering.
568 Geotext. and Geomembr. 28(5), 475-482.

569 Zhang, L., Zhao, M., Zou, X., Zhao, H. 2010b. Analysis of geocell-reinforced mattress with consideration of horizontal–
570 vertical coupling. Comput. Geotech. 37 (6), 748–756.

571 Zhang, L., Qiangkang, Gu., Guoping, Cen., 2010c. Effect of Geo-Cell Reinforced Soil Structure Used in Flexible Airfield
572 Pavement. iclem logistics for sustained economic development, ASCE. 1629-1635.

573 Zhou, H.B., Wen, X.J., 2008. Model studies on geogrid- or geocell-reinforced sand mattress on soft soil. Geotext.
574 Geomembr. 26(3), 231–238.

575 Nomenclature

a	Loading plate radius *(m)*
b	Width of the geocell layers *(m)*
a_1, a_2, b_1 *and* b_2	Model parameters to estimate the elastic modulus of gocell-reinforced layers
D	Loading plate diameter *(m)*
D_f	Embedment depth of footing *(m)*
E_g	Elastic modulus of layer of geocell and soil *(kPa)*
E_H	Equivalent elastic modulus of upper soil layer of thickness *H (kPa)*
E_i, E_j, E_m, E_n	Elastic modulus of layer *i, j, m, n (kPa)*
$f(\varepsilon)$	Function to consider the strain level in estimating the elastic modulus of unreinforced and geocell-reinforced layers
H_e	Equivalent thickness *(m)*
H_{1e}	Equivalent thickness of the first layer *(m)*
H_{me}	Equivalent thickness of the m^{th} layer *(m)*
H_{eff}	Effective depth *(m)*
H_{ie}	Equivalent thickness of the each layer *(m)*
h_g	Height of geocell layers *(m)*
H_m	Thickness of m^{th} layer *(m)*
h_s	Vertical spacing of the geocell layers *(m)*
k_r	Lateral pressure coefficient for geocell-reinforced layers
K_u	Dimensionless modulus number of the unreinforced sand in the hyperbolic model
k_{un}	Lateral pressure coefficient for unreinforced layers
M	Secant tensile modulus of the geocell material at an average strain of 2.5% *(kN/m)*
MLE	Multiple Linear Elastic
n	Number of layers of multilayered system
N_g	Number of geocell layers
u	Vertical distance of the first layer of geocell from the footing *(m)*

q	Uniform pressure on a circular footing with radius "a" *(kPa)*
w	Actual total surface settlement at the center of the circular loading surface *(m)*
w^{j}	Vertical displacement at surface of system for loading of q_j *(m)*
w_0	Vertical deflection at the center of loading on surface (at depth of z=0) of uniform equivalent layer *(m)*
w_1	Vertical deflection at bottom of the equivalent layer *(m)*
w_i	Vertical deflection on top of ith equivalent layer *(m)*
w_{pi}	Vertical thinning of i^{th} original layer with thickness of H_i *(m)*
w_2	Vertical thinning of the original layer with thickness of H *(m)*
z	Depth of the backfill *(m)*
Δw	Vertical deformation (thinning) increment *(m)*
Δw_i^j	Displacement increment of equivalent layer for i^{th} layer *(m)*
$(\Delta w_p)_i^j$	Deformation increment (thinning) of layer with thickness of H_i for loading increment q_j-q_{j-1} *(m)*
Δw_1^j	Vertical displacement increment on loading centerline at a depth of H_e for loading increment of q_j-q_{j-1} *(m)*
Δw_0^j	Vertical displacement increment at surface (of equivalent layer) beneath centre of load for loading increment of q_j-q_{j-1} *(m)*
Δw_2^j	Vertical deformation (thinning) increment of the original layer of thickness of H *(m)*
ε_i	Strain across the thickness of the i^{th} layer *(%)*
ε_i^j	Strain of layer with thickness of H_i subjected to loading q_j *(%)*
φ	Angle of shearing resistance of soil being reinforced *(degree)*
v_n	Poisson's ratio of layer n
σ_d	Deviatoric stress *(kPa)*
σ_1	Vertical stress *(kPa)*
σ_3	Confining pressure *(kPa)*

576

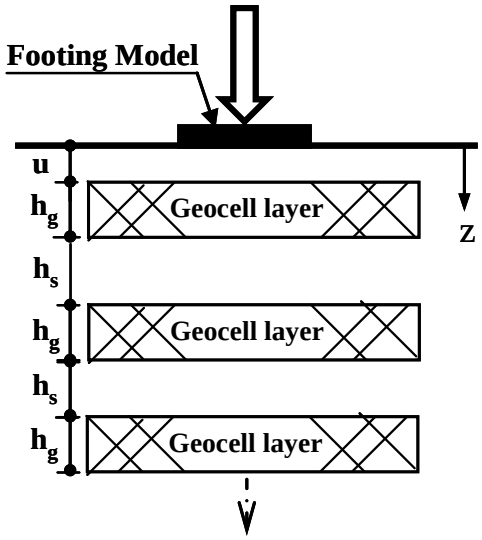

Fig. 1. Schematic of multi-layered geocell-reinforced foundation bed

577

578

579

580

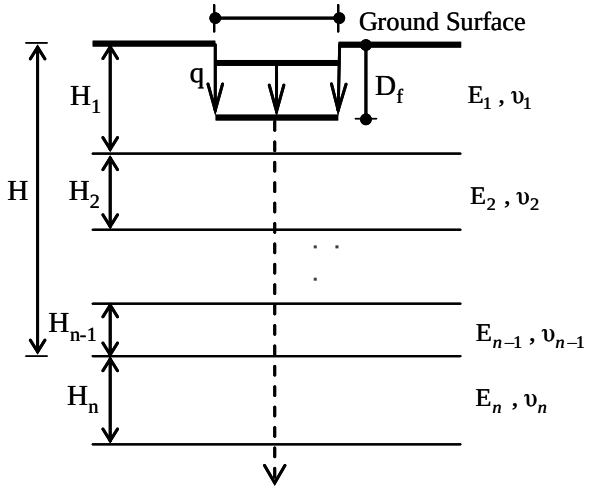

Fig. 2. Multi-layered soil systems (Hirai, 2008)

581

582

583

584

585

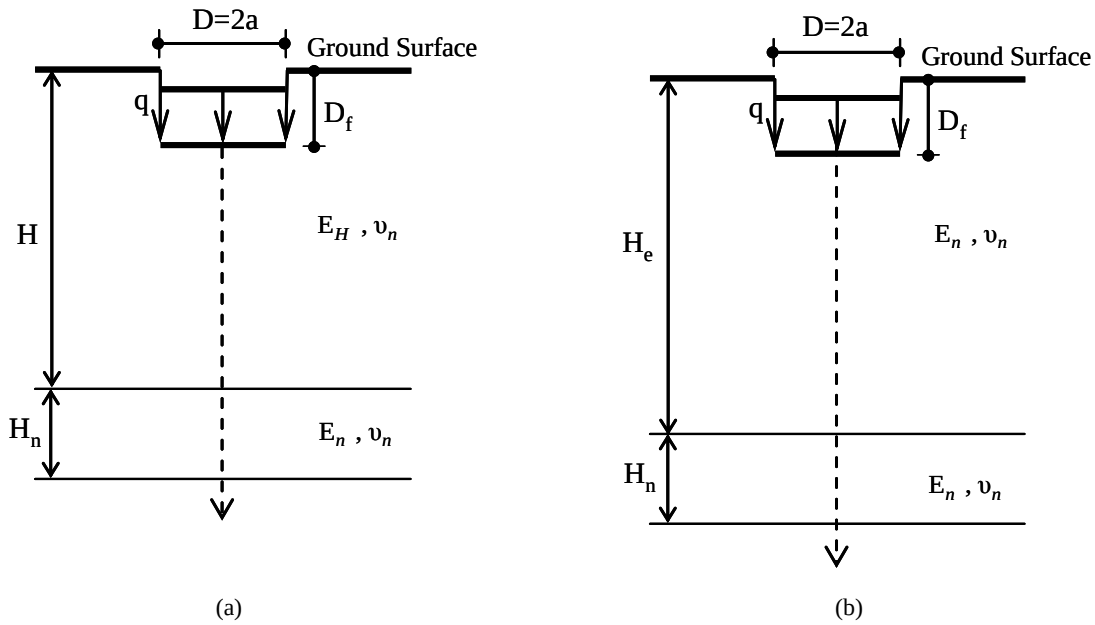

Fig. 3. (a) Equivalent two-layered soil system for Fig. 2 (b) Equivalent single layer soil system with the same E_n and v_n for Fig. 3a. (Hirai, 2008)

586

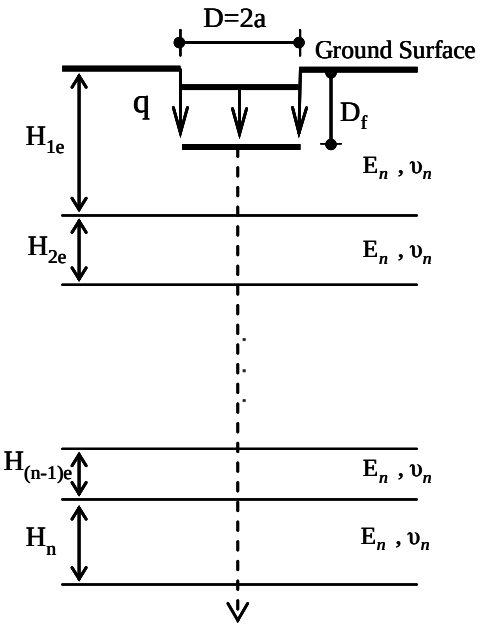

Fig. 4. Equivalent single soil layer with equivalent thickness of "H_{1e}+H_{2e}+H_{3e}+…. + $H_{(n\text{-}1)e}$+H_n" and E_n and v_n for Fig. 2 (Hirai, 2008)

587

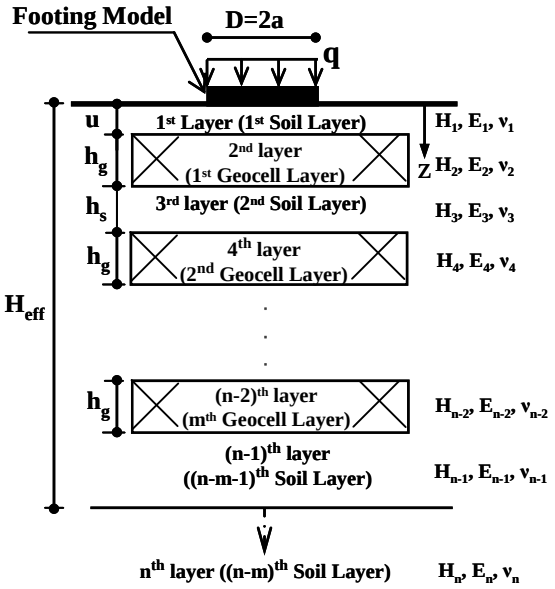

Fig. 5. "n" layer geocell-reinforced soil system containing "m" layers of geocell.

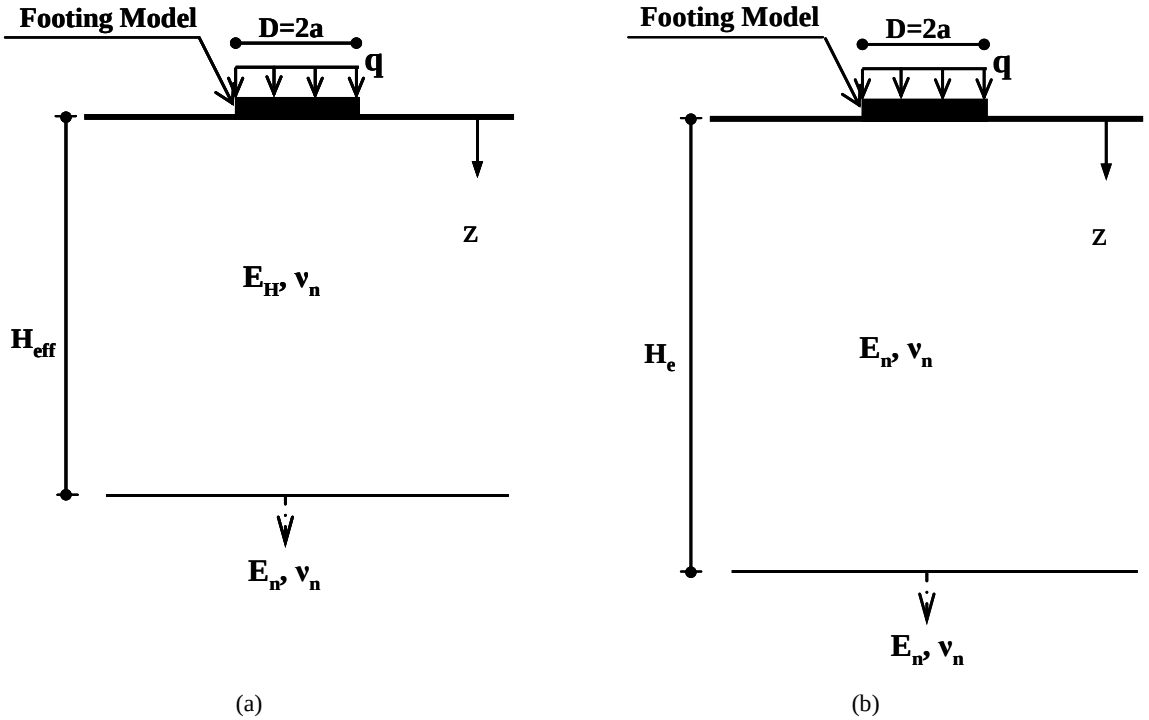

Fig. 6. Substituting n-layer system sequentially with (a) Equivalent two-layered system for n-layer system in Fig. 5 (b) Equivalent single layer system with the same E_n and ν_n for two-layered system in Fig. 6a.

598

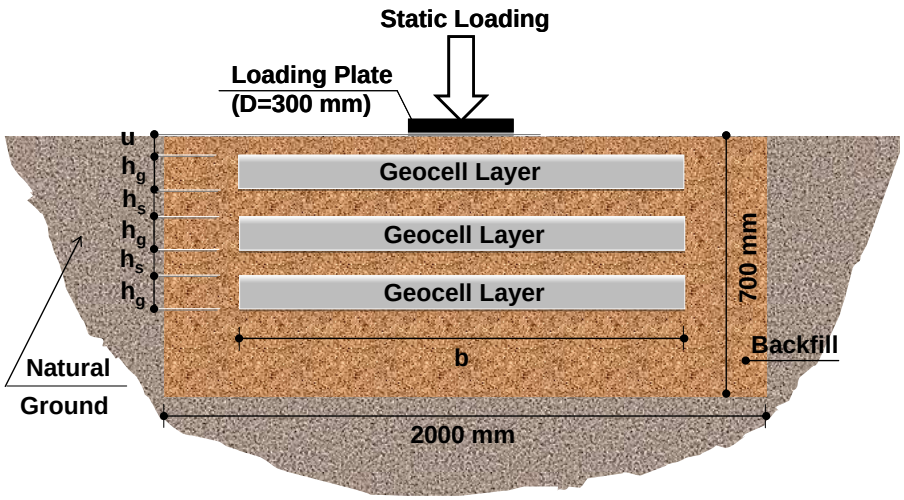

Fig. 7. Geometry of the test configurations used to validate the results of the method presented (D=300 mm, $u=h_s=0.2D$=60 mm, h_g=100 mm and $b/D=5$ (Moghaddas Tafreshi et al., 2013)).

599

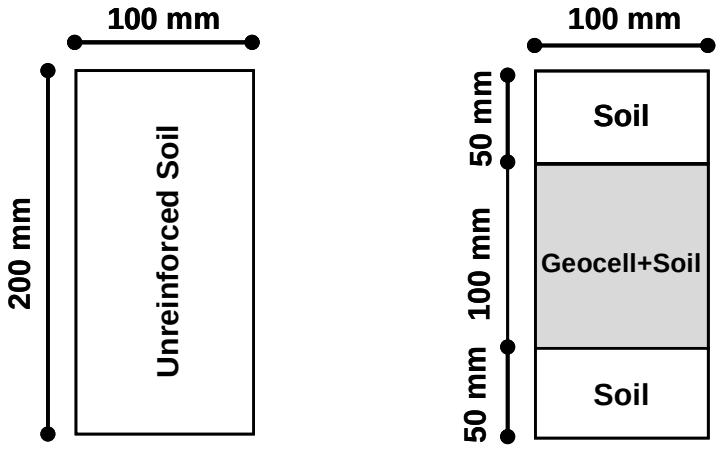

(a) (b)

Fig. 8. Configurations used in triaxial tests (a) unreinforced (b) reinforced with one layer of geocell (Noori, 2012).

600

601

602

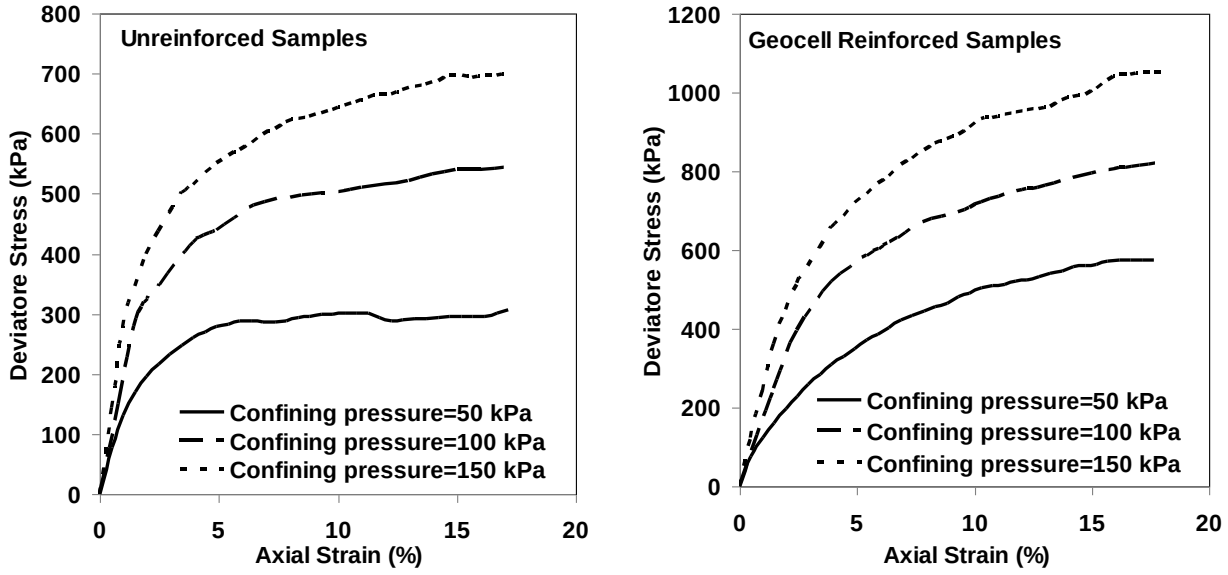

(a) (b)

Fig. 9. Stress-axial strain curves for unreinforced and geocell reinforced samples under confining pressure of 50, 100 and 150 kPa (a) unreinforced samples, (b) geocell reinforced samples (Noori, 2012).

603

604

605

606

607

608

609

610

611

612

613

614

615

616

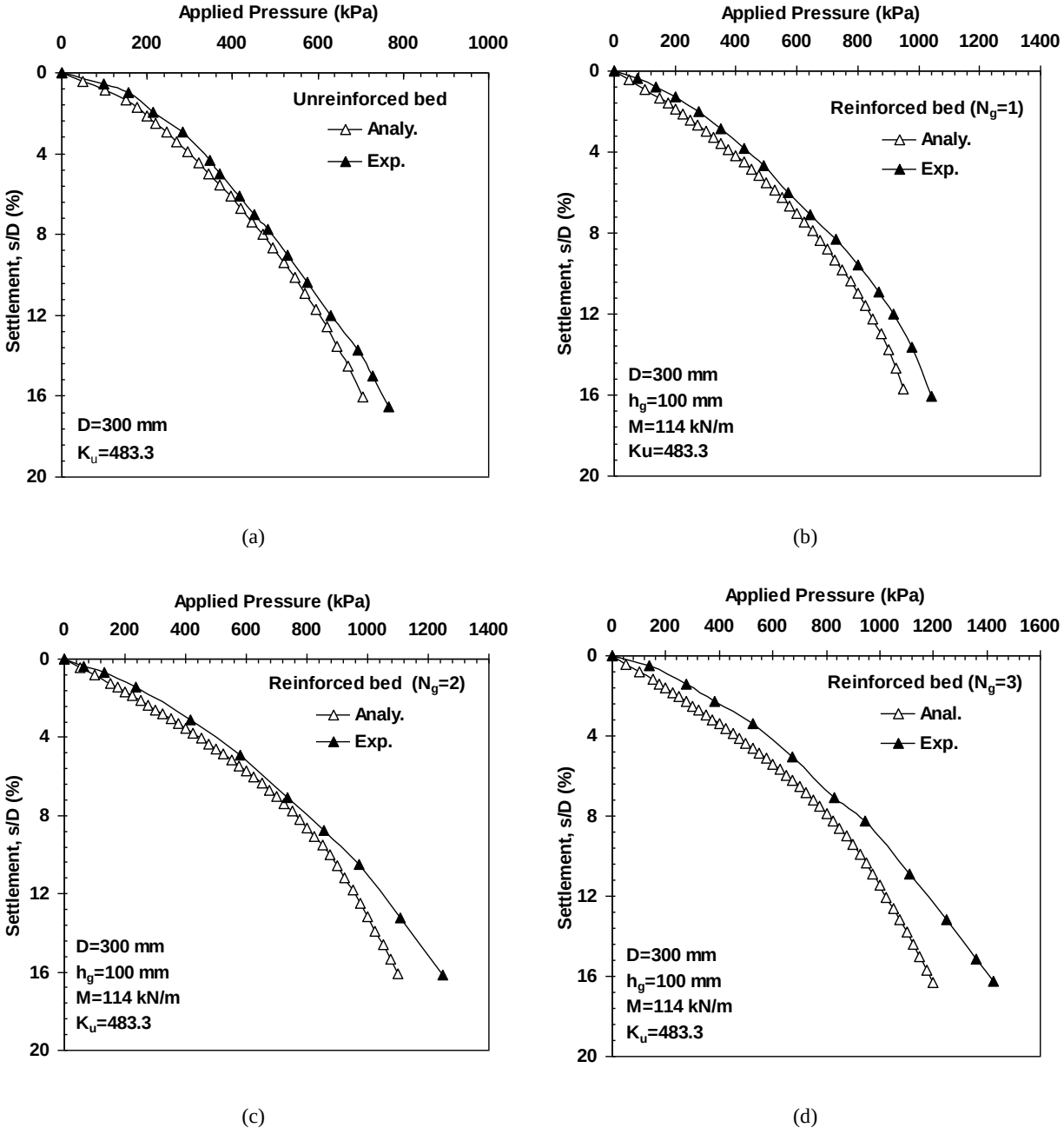

Fig. 10. Comparison of analytical and experimental results for (a) unreinforced bed, (b) reinforced bed with one layer of geocell, (c) reinforced bed with two layers of geocell, (d) reinforced bed with three layers of geocell

617

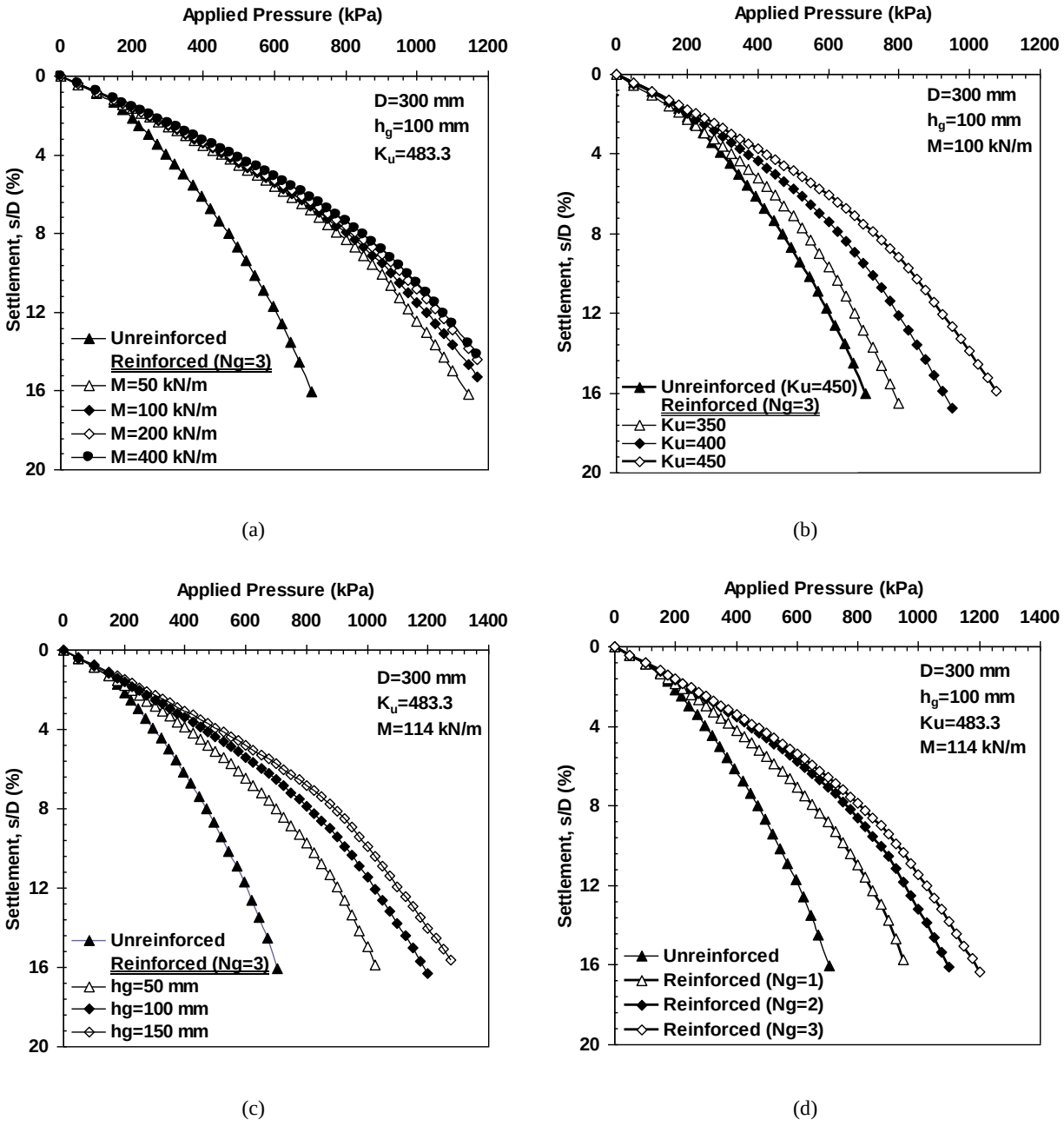

Fig. 11. Variation of pressure-settlement response of geocell-reinforced bed for different (a) secant modulus of geocell (M), (b) soil dimensionless modulus (K_u), (c) thickness of geocell layers (h_g), and (d) number of geocell layers (N_g)

618

619

620

621

622